8 Cross-Sectional Microscopic Anatomy of the Brachial Plexus and Paraneural Sheaths

Miguel Angel Reina and Xavier Sala-Blanch

Ultrasound allows visualization of nerve trunks and branches to guide the position of the needle during anesthetic blockade. Although image resolution of newer ultrasound devices is much better than the resolution of earlier equipment, the invaluable contribution of histological techniques and the relevance of the morphological features they reveal cannot be refuted.

In this regard, details of the type and size of fascicles inside nerves achieved with current ultrasound equipment do not match those obtained by histological methods. There is lack of correlation between ultrasound images and the real anatomy of nerve fascicles. In addition, images of fascicles visualized in a histological section do not match ultrasound images of the same nerve in the same location.

Sectional anatomy aids in the interpretation of images obtained by ultrasound, although it is rare for cross sections to accurately match the orientation of the section produced with the ultrasound probe. At the level of the brachial plexus, ultrasound sections are typically transversal to the direction of the trunks and nerve branches.

The aim of this chapter is to present histological images from real anatomic sections at an anatomical level identical to that of ultrasound images obtained during anesthetic blockade. The resulting images enable accurate identification of microscopic features of anatomical structures identified by ultrasound imaging, as well as structures that are too small to be seen in ultrasound images [1–6]. Sections of this type also allow precise identification of connective tissue enclosing different structures comprising the brachial plexus, including paraneural layers that form several compartments containing fat and small vessels (Figs. 8.1, 8.2, 8.3, 8.4, 8.5, 8.6, 8.7, 8.8, 8.9, 8.10, 8.11, 8.12, 8.13, 8.14, 8.15, 8.16, 8.17, 8.18, 8.19, 8.20, 8.21, 8.22, 8.23, 8.24, 8.25, and 8.26). Figures 8.1–8.23 are images of successive sections from same cadaver, from interscalenic region to axillary region.

M.A. Reina, MD, PhD (✉)
Department of Clinical Medical Sciences and Institute of Applied Molecular Medicine, School of Medicine, University of CEU San Pablo, Madrid, Spain

Department of Anesthesiology, Madrid-Montepríncipe University Hospital, Madrid, Spain
e-mail: miguelangel@perticone.e.telefonica.net

X. Sala-Blanch, MD
Human Anatomy and Embryology Unit, School of Medicine, University of Barcelona, Barcelona, Spain

Department of Anesthesiology and Critical Care, Clinic Hospital, Barcelona, Spain
e-mail: xavi.sala.blanch@gmail.com

M.A. Reina et al. (eds.), *Atlas of Functional Anatomy for Regional Anesthesia and Pain Medicine: Human Structure, Ultrastructure and 3D Reconstruction Images*, DOI 10.1007/978-3-319-09522-6_8,

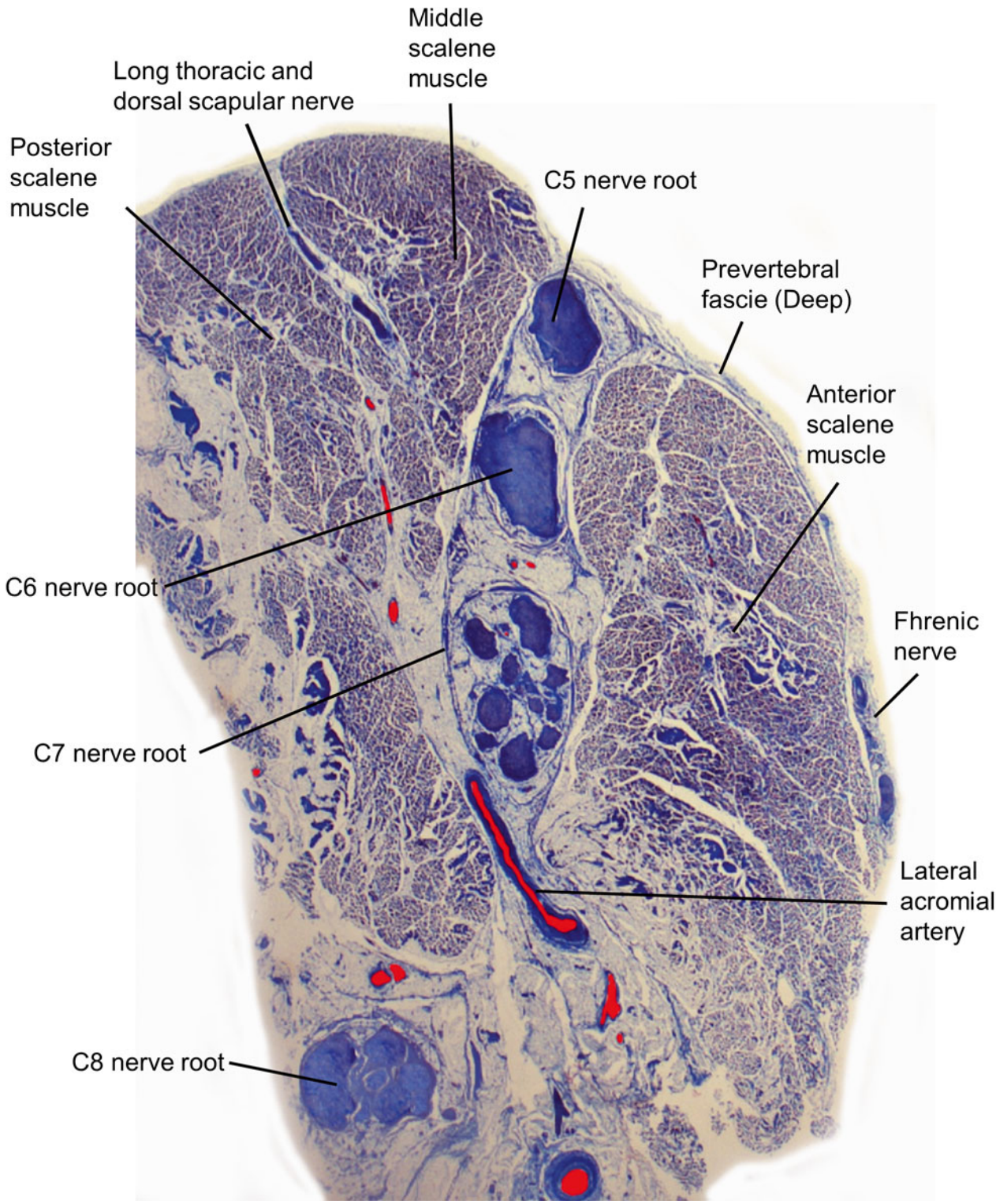

Fig. 8.1 Brachial plexus, interscalenic region. Masson's trichrome stained. First section of a serially sectioned sample

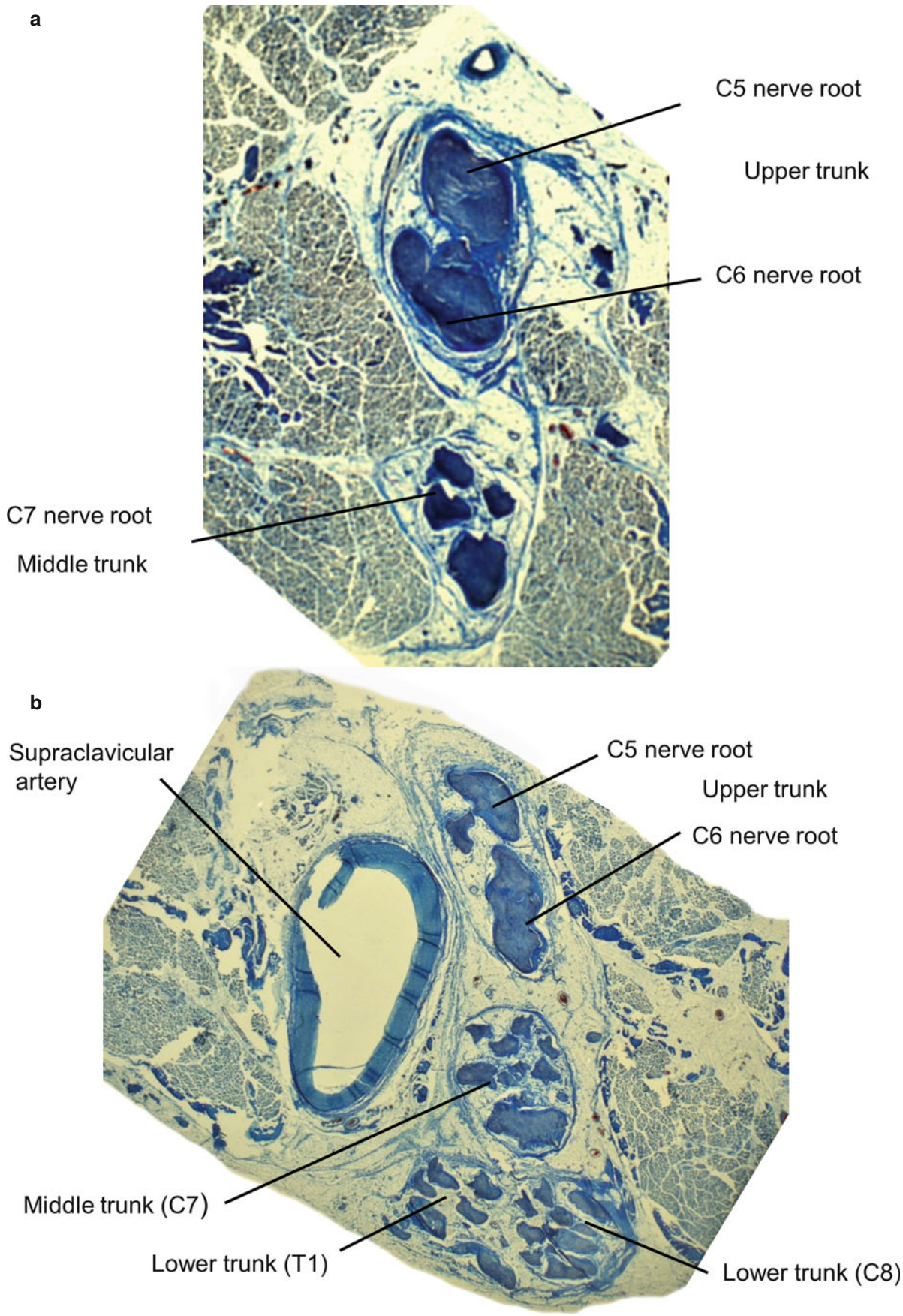

Fig. 8.2 Brachial plexus, interscalenic region. (**a**) and (**b**) are two successive sections. Masson's trichrome stained. Following section of a serially sectioned sample from Figs. 8.1 to 8.23

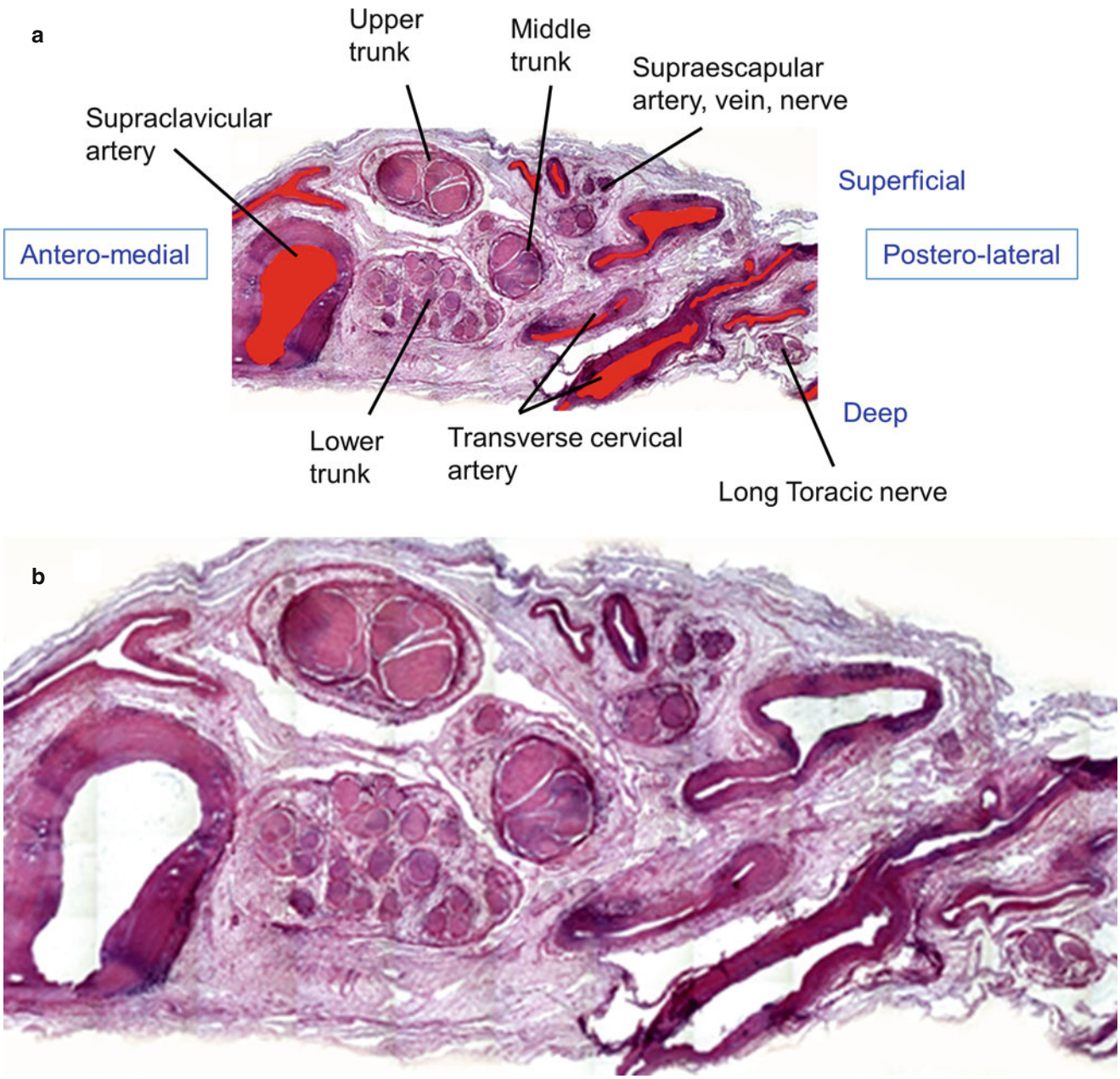

Fig. 8.3 (**a**) Brachial plexus, supraclavicular region. (**b**): (**a**) at more magnification. Hematoxylin-eosin stained. Following section of a serially sectioned sample from Figs. 8.1 to 8.23

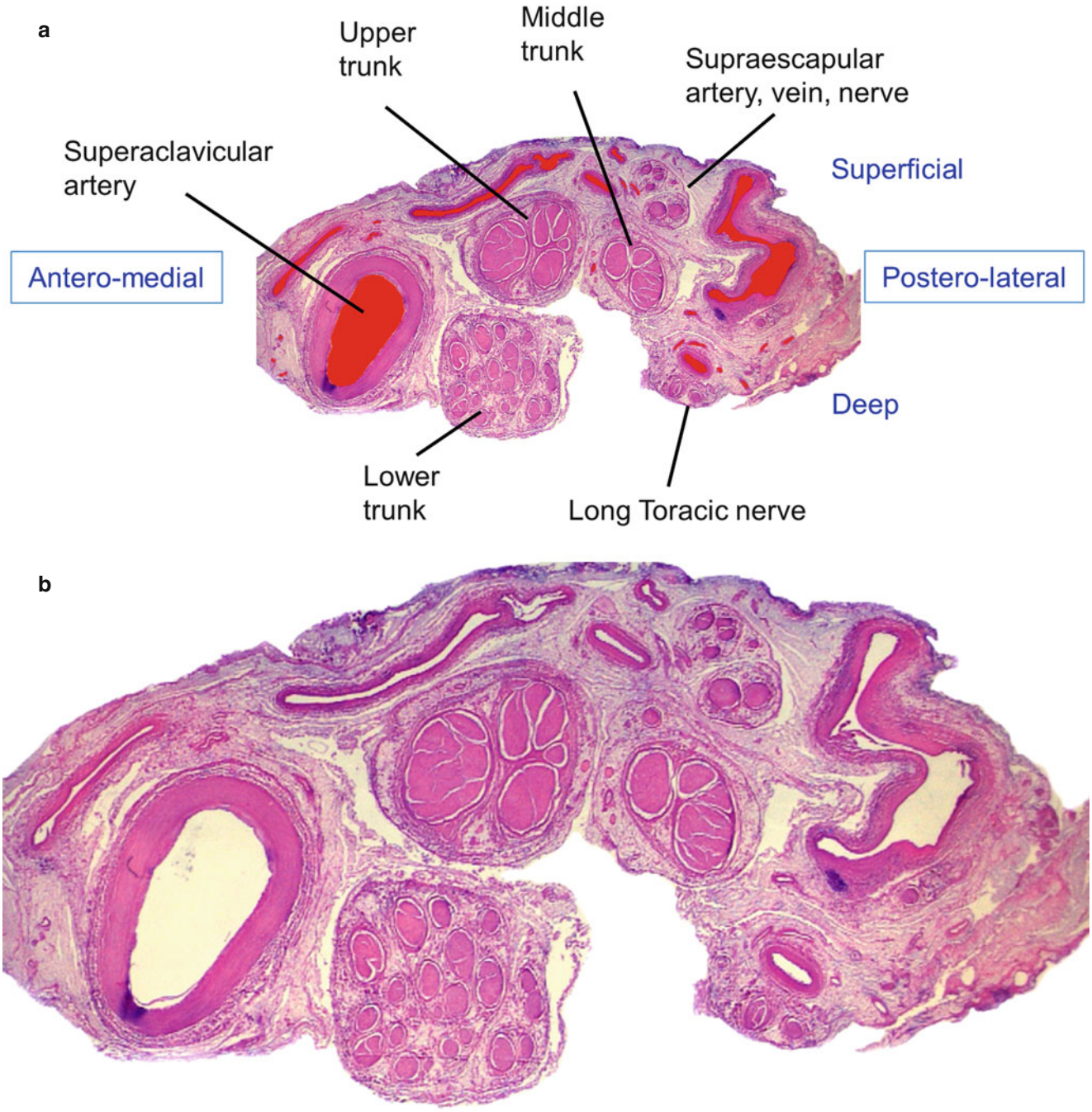

Fig. 8.4 (**a**) Brachial plexus, supraclavicular region. (**b**): (**a**) at more magnification. Hematoxylin-eosin stained. Following section of a serially sectioned sample from Figs. 8.1 to 8.23

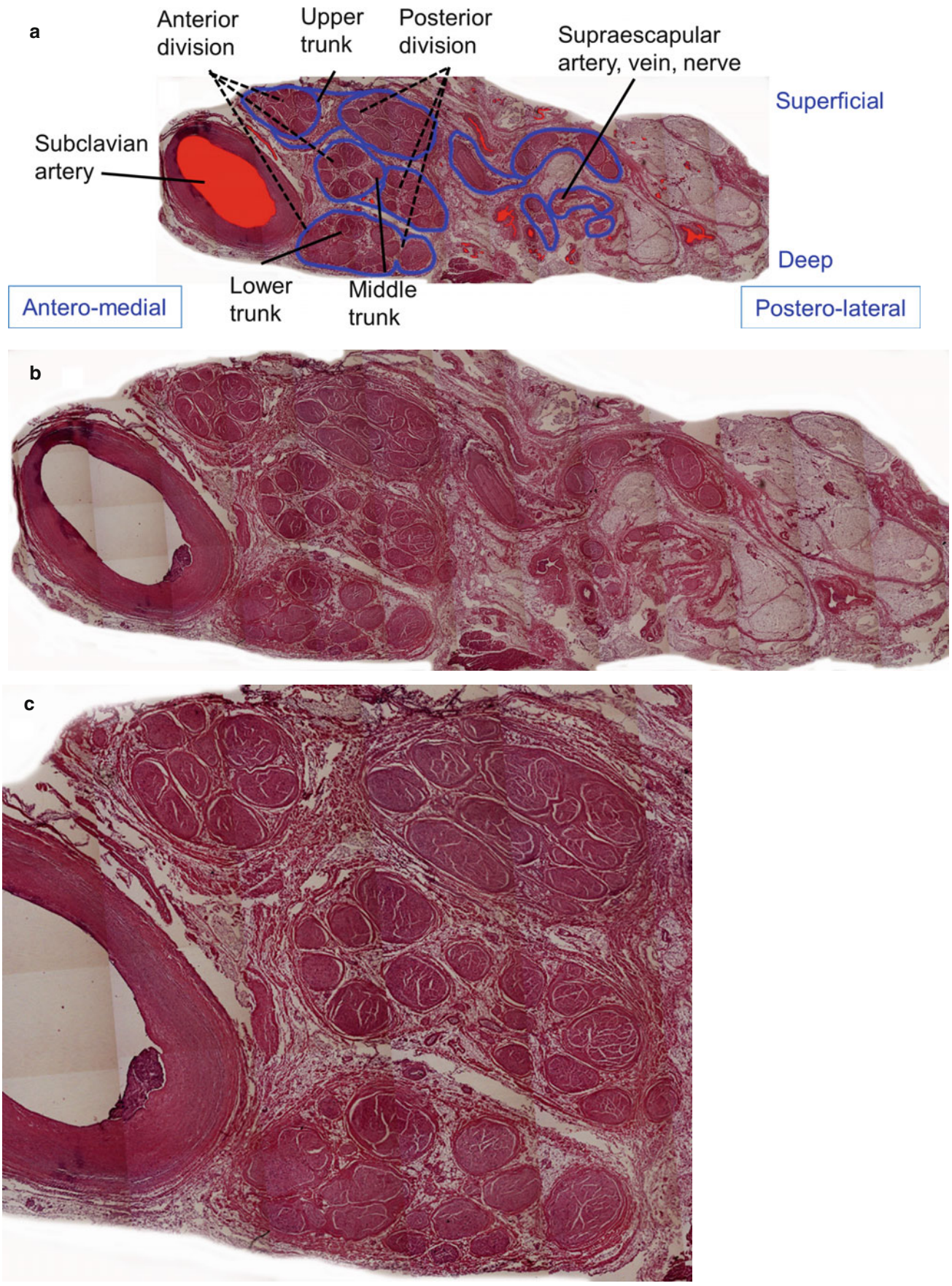

Fig. 8.5 (**a**) Brachial plexus, supraclavicular region. (**b**): (**a**) at more magnification. (**c**) Detail of (**b**). Hematoxylin-eosin stained. Following section of a serially sectioned sample from Figs. 8.1 to 8.23

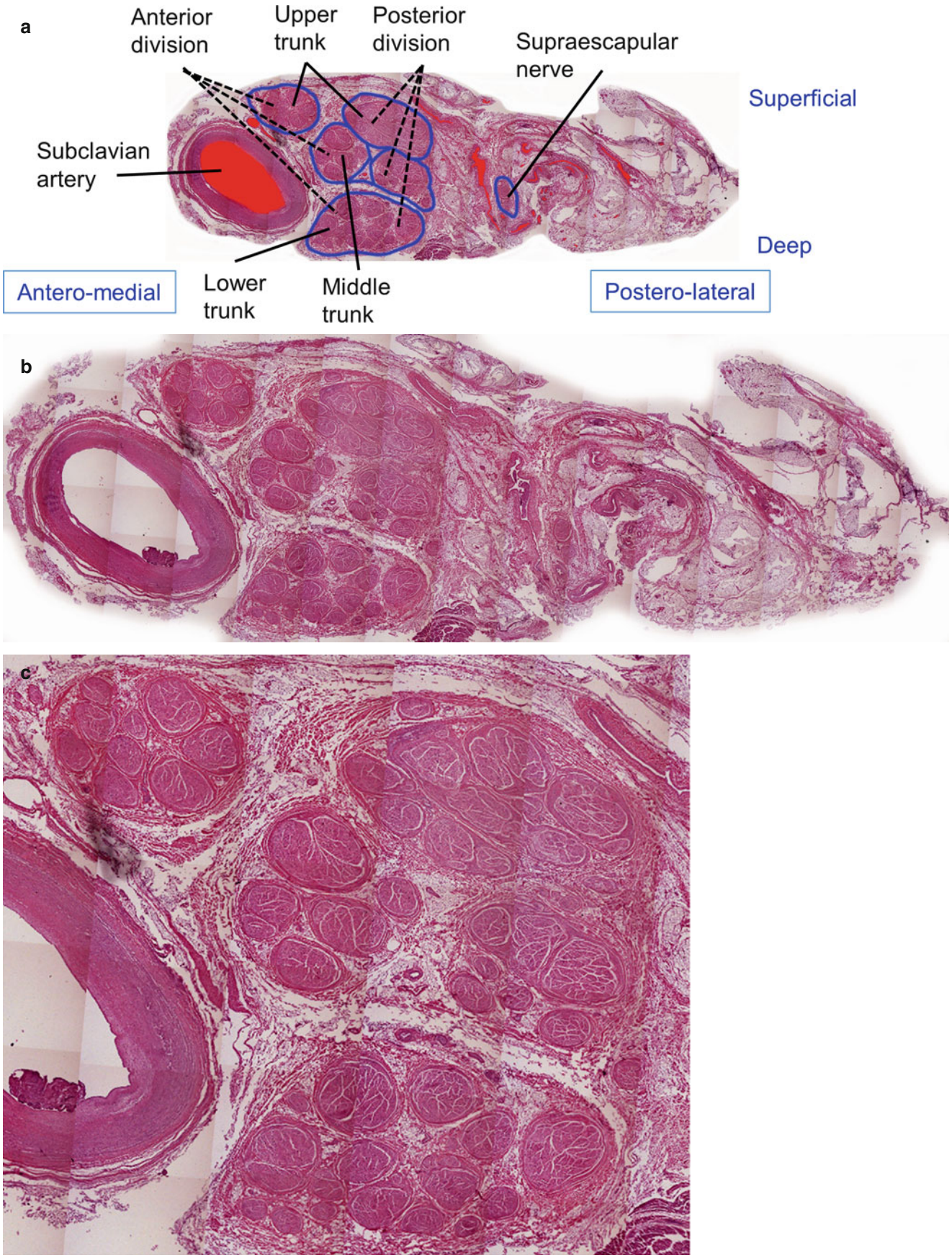

Fig. 8.6 (**a**) Brachial plexus, supraclavicular region at retroclavicular level. (**b**): (**a**) at more magnification. (**c**) Detail of (**b**). Hematoxylin-eosin stained. Following section of a serially sectioned sample from Figs. 8.1 to 8.23

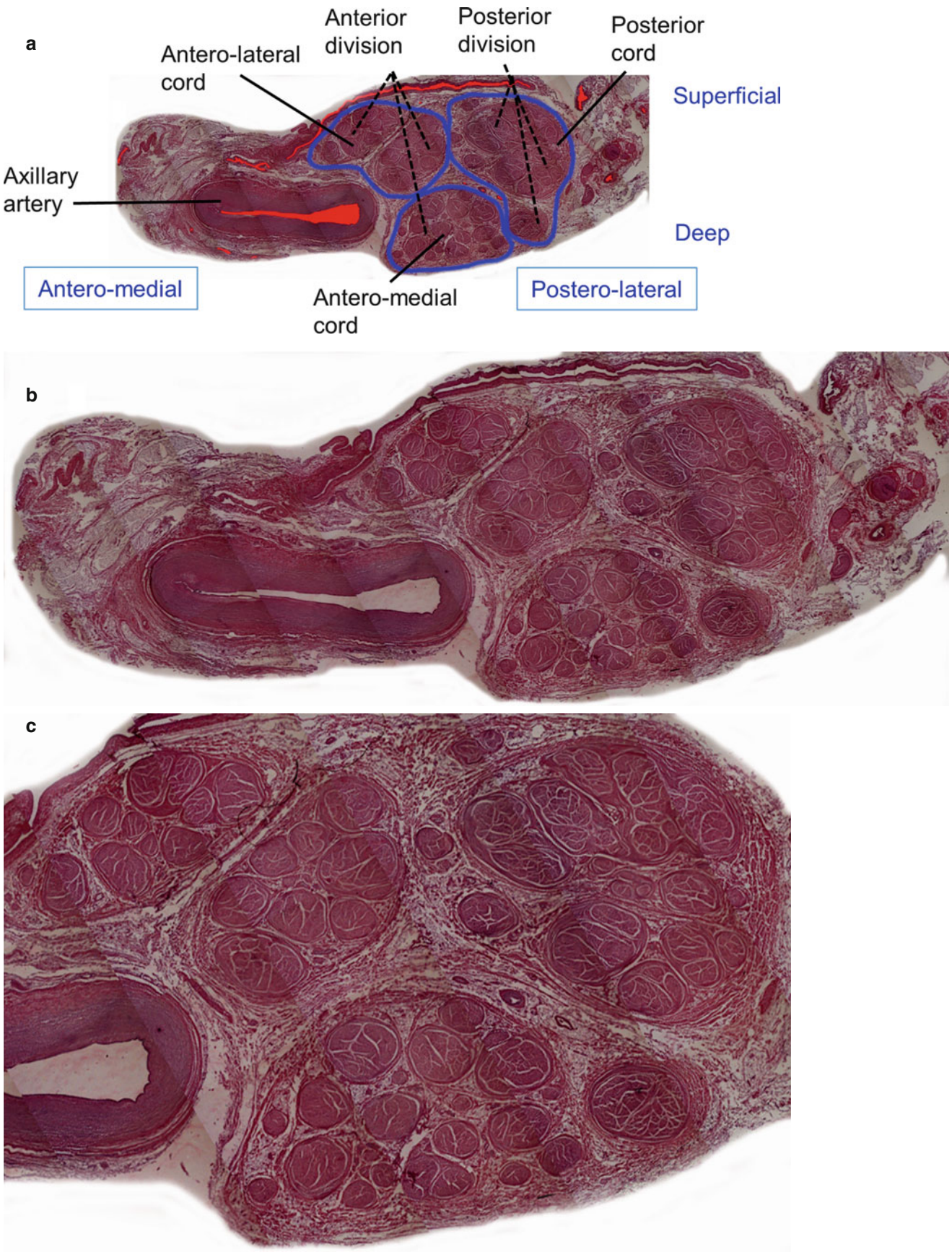

Fig. 8.7 (**a**) Brachial plexus, supraclavicular region at retroclavicular level. (**b**): (**a**) at more magnification. (**c**) Detail of (**b**). Hematoxylin-eosin stained. Following section of a serially sectioned sample from Figs. 8.1 to 8.23

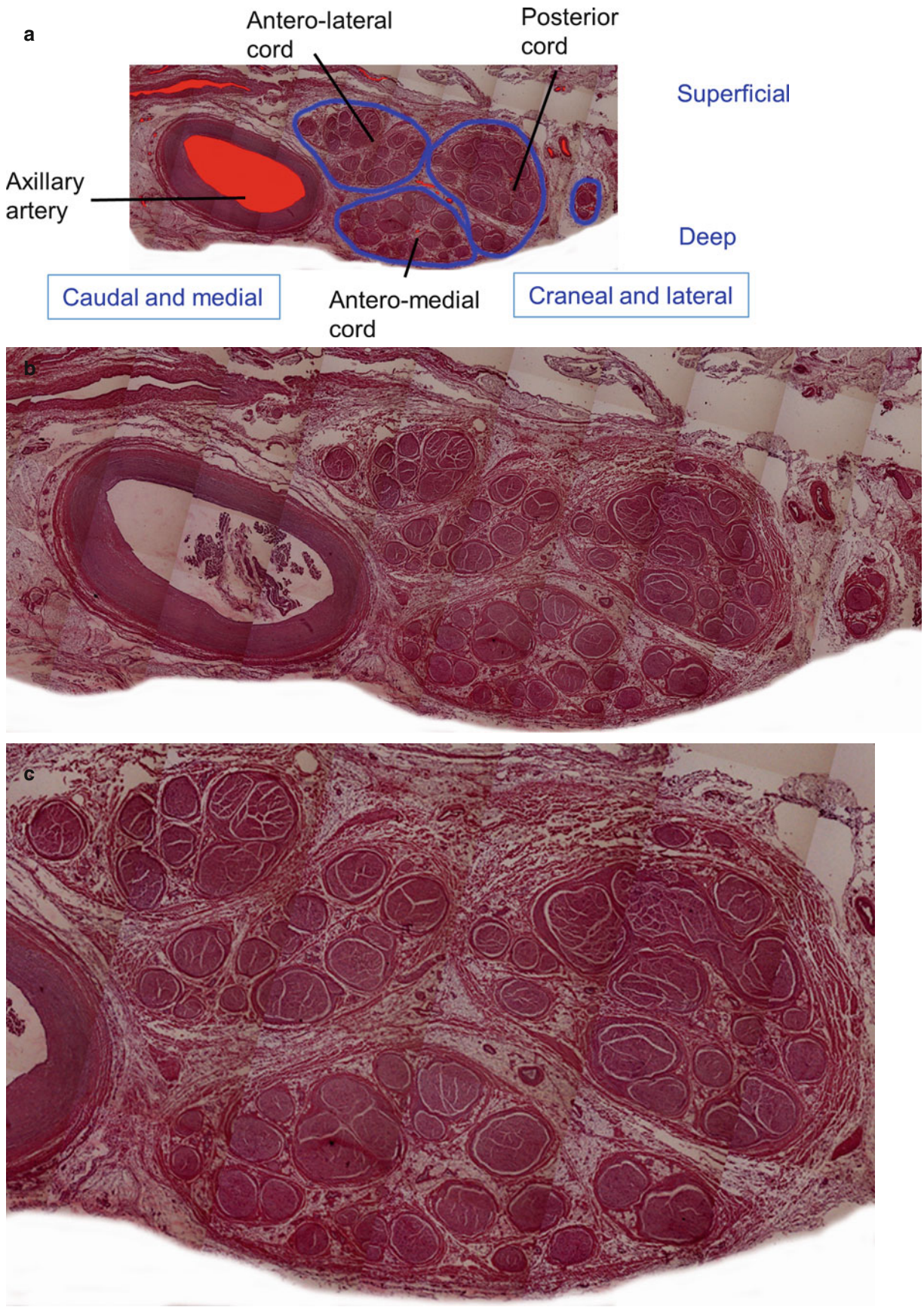

Fig. 8.8 (**a**) Brachial plexus, infraclavicular region. Hematoxylin-eosin stained. (**b**): (**a**) at more magnification. (**c**) Detail of (**b**). Following section of a serially sectioned sample from Figs. 8.1 to 8.23

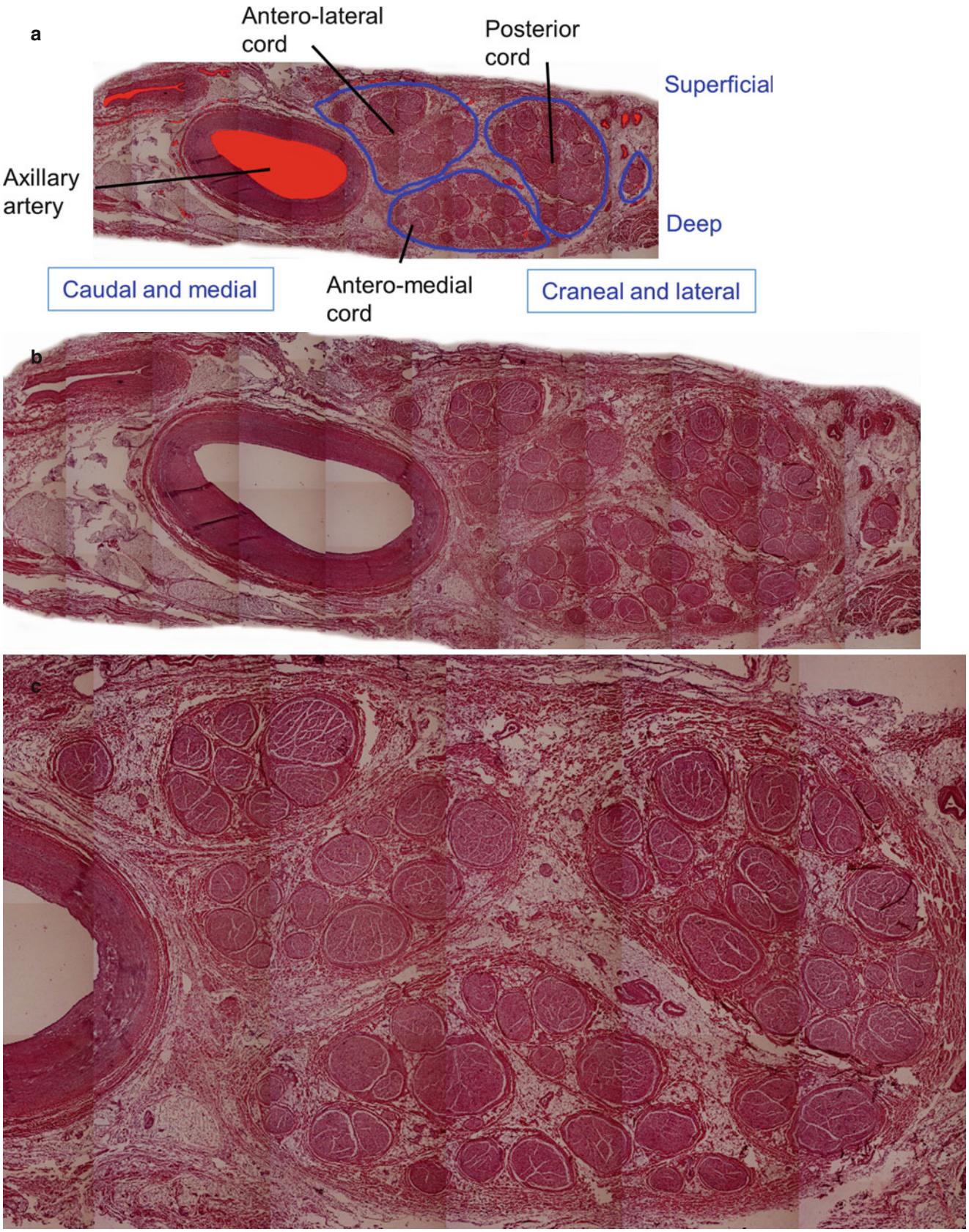

Fig. 8.9 (**a**) Brachial plexus, infraclavicular region at first part level. (**b**): (**a**) at more magnification. (**c**) Detail of (**b**). Hematoxylin-eosin stained. Following section of a serially sectioned sample from Figs. 8.1 to 8.23

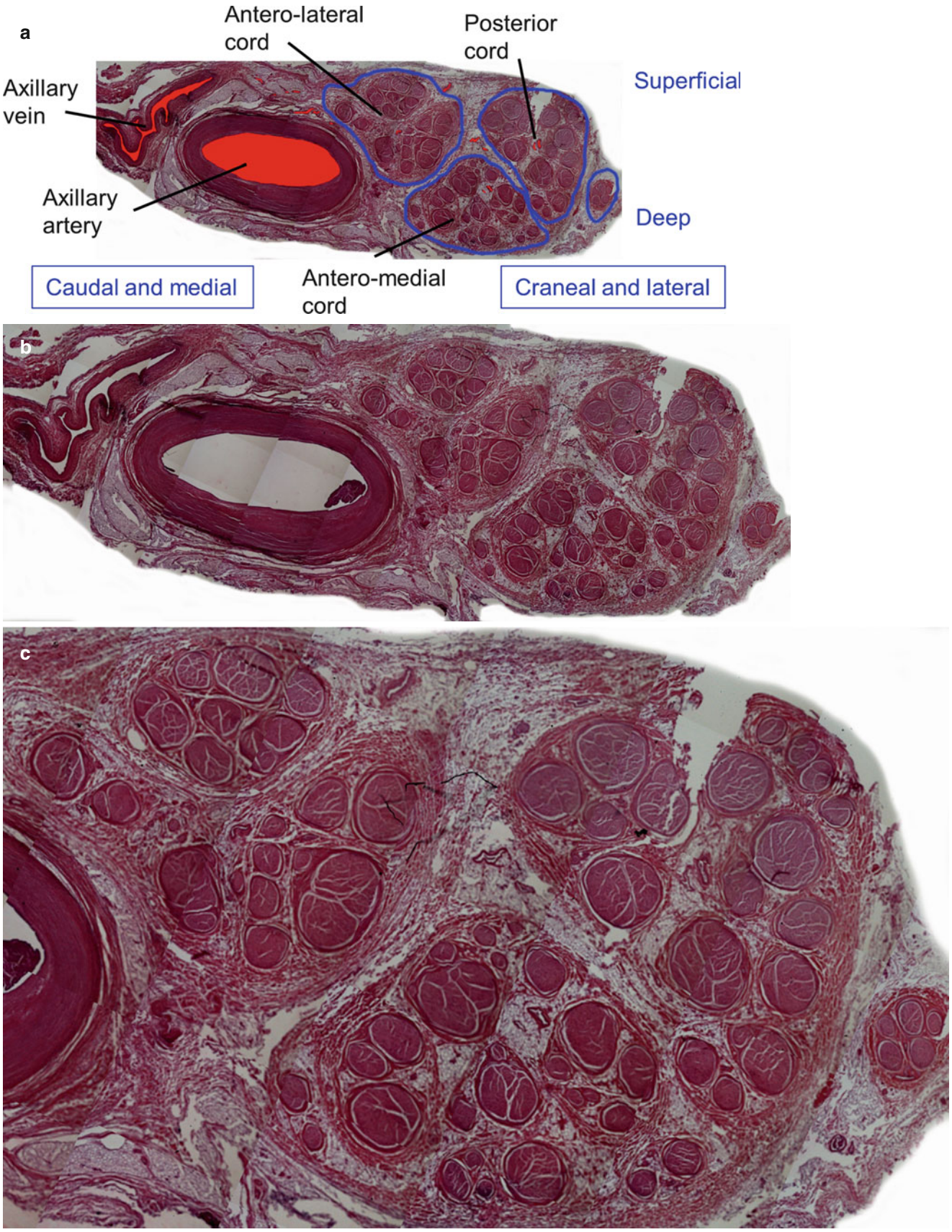

Fig. 8.10 (**a**) Brachial plexus, infraclavicular region at first part level. (**b**): (**a**) at more magnification. (**c**) Detail of (**b**). Hematoxylin-eosin stained. Following section of a serially sectioned sample

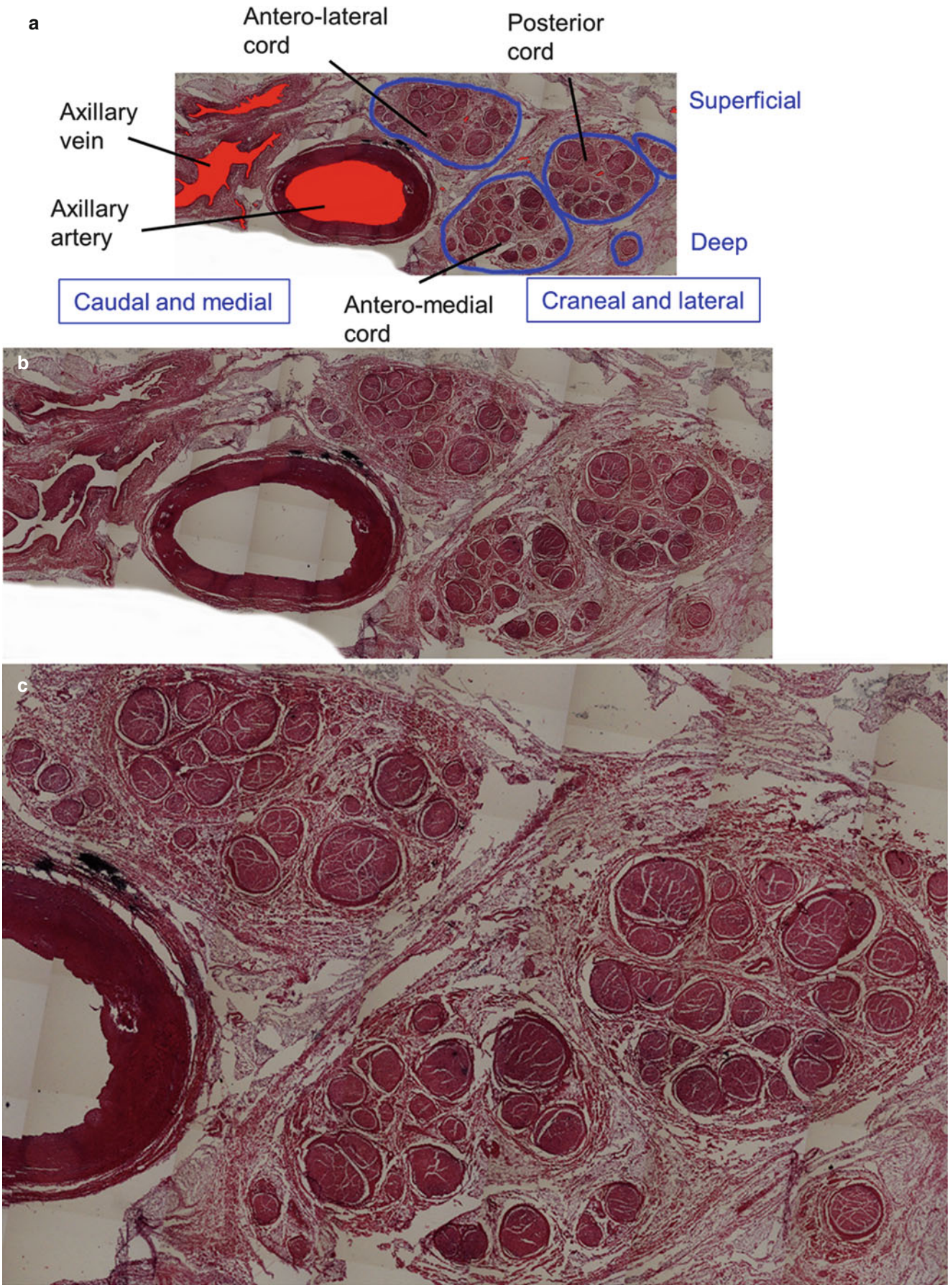

Fig. 8.11 (**a**) Brachial plexus, infraclavicular region at first part level. (**b**): (**a**) at more magnification. (**c**) Detail of (**b**). Hematoxylin-eosin stained. Following section of a serially sectioned sample from Figs. 8.1 to 8.23

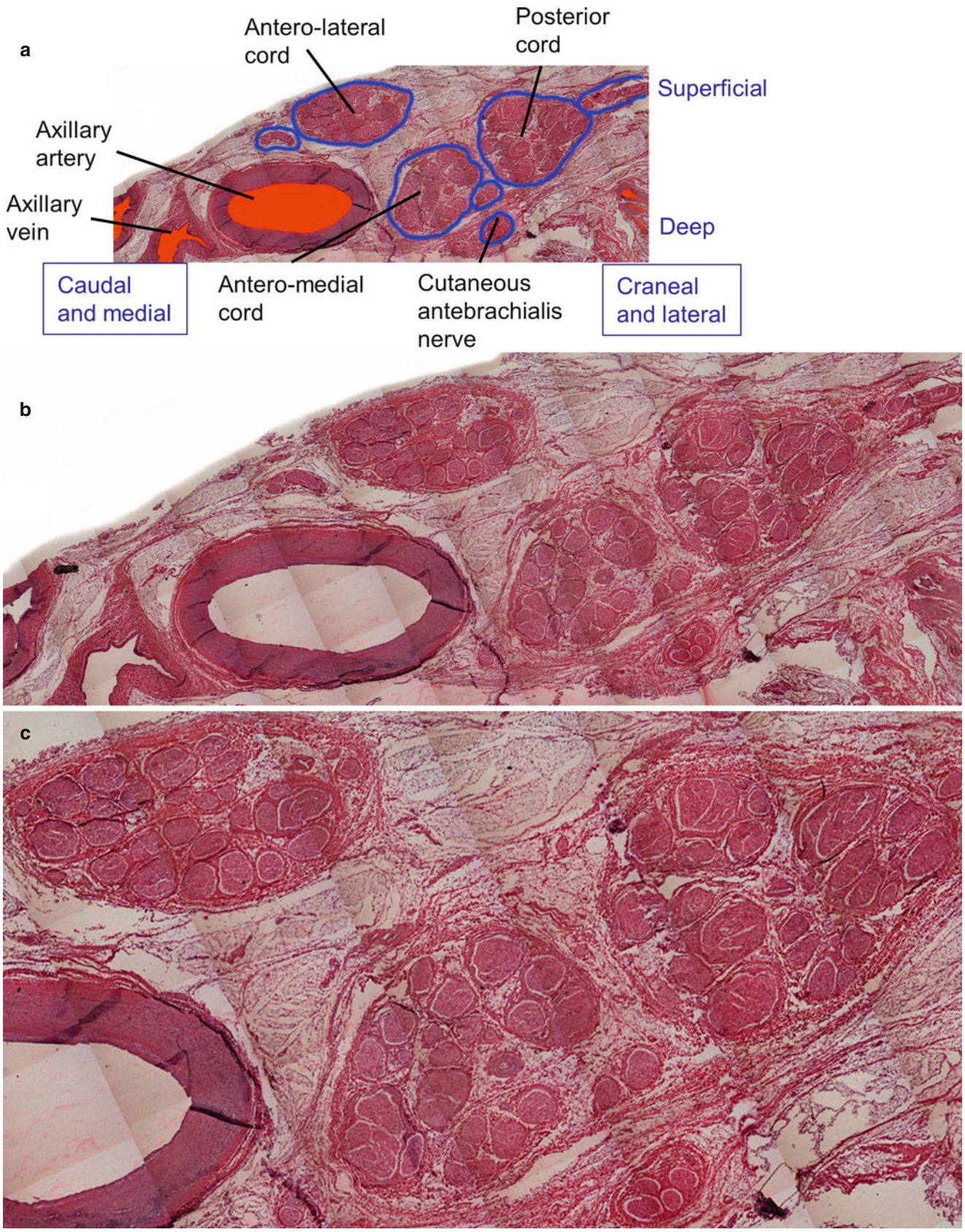

Fig. 8.12 (**a**) Brachial plexus, infraclavicular region at first part level. (**b**): (**a**) at more magnification. (**c**) Detail of (**b**). Hematoxylin-eosin stained. Following section of a serially sectioned sample from Figs. 8.1 to 8.23

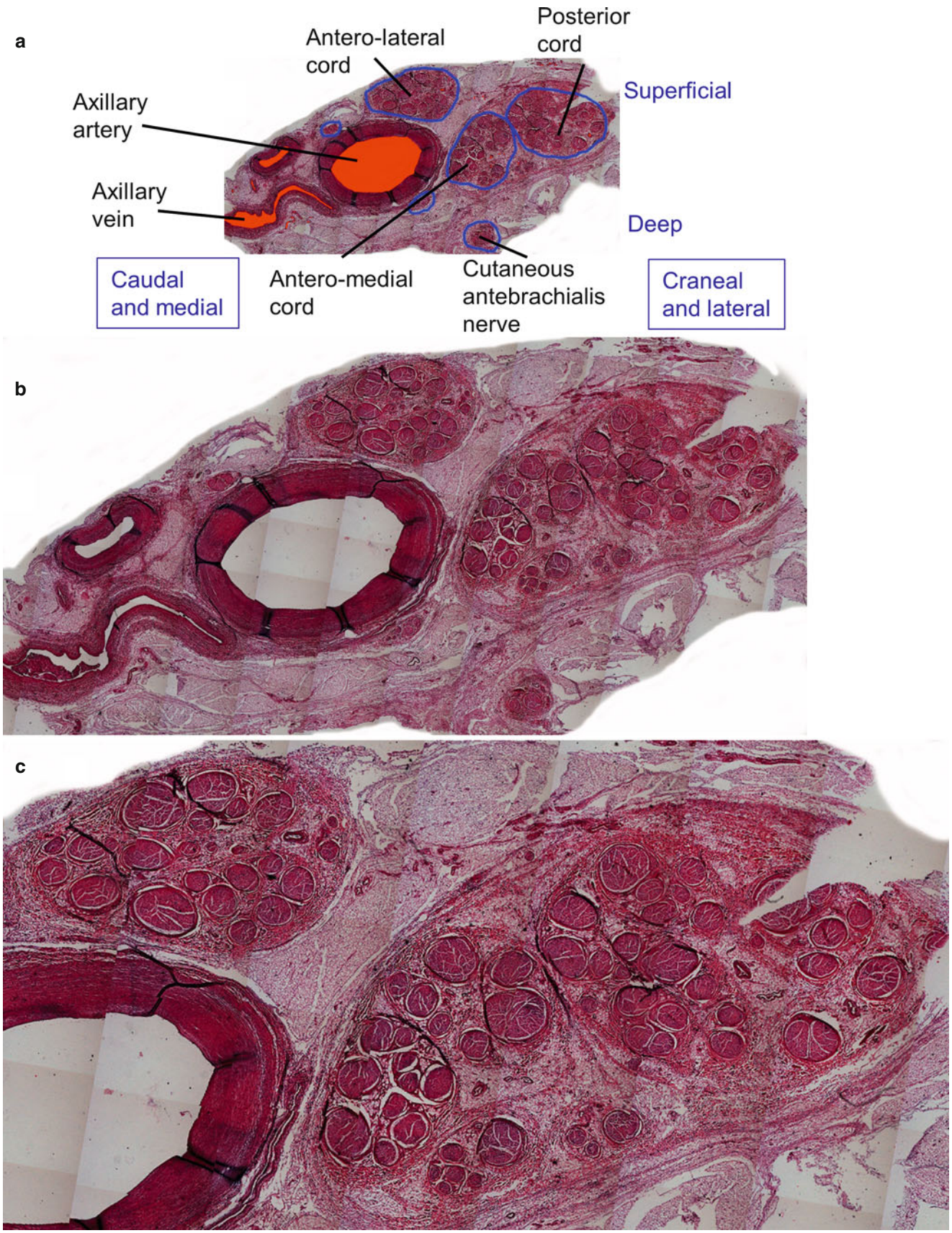

Fig. 8.13 (**a**) Brachial plexus, infraclavicular region at first part level. (**b**): (**a**) at more magnification. (**c**) Detail of (**b**). Hematoxylin-eosin stained. Following section of a serially sectioned sample from Figs. 8.1 to 8.23

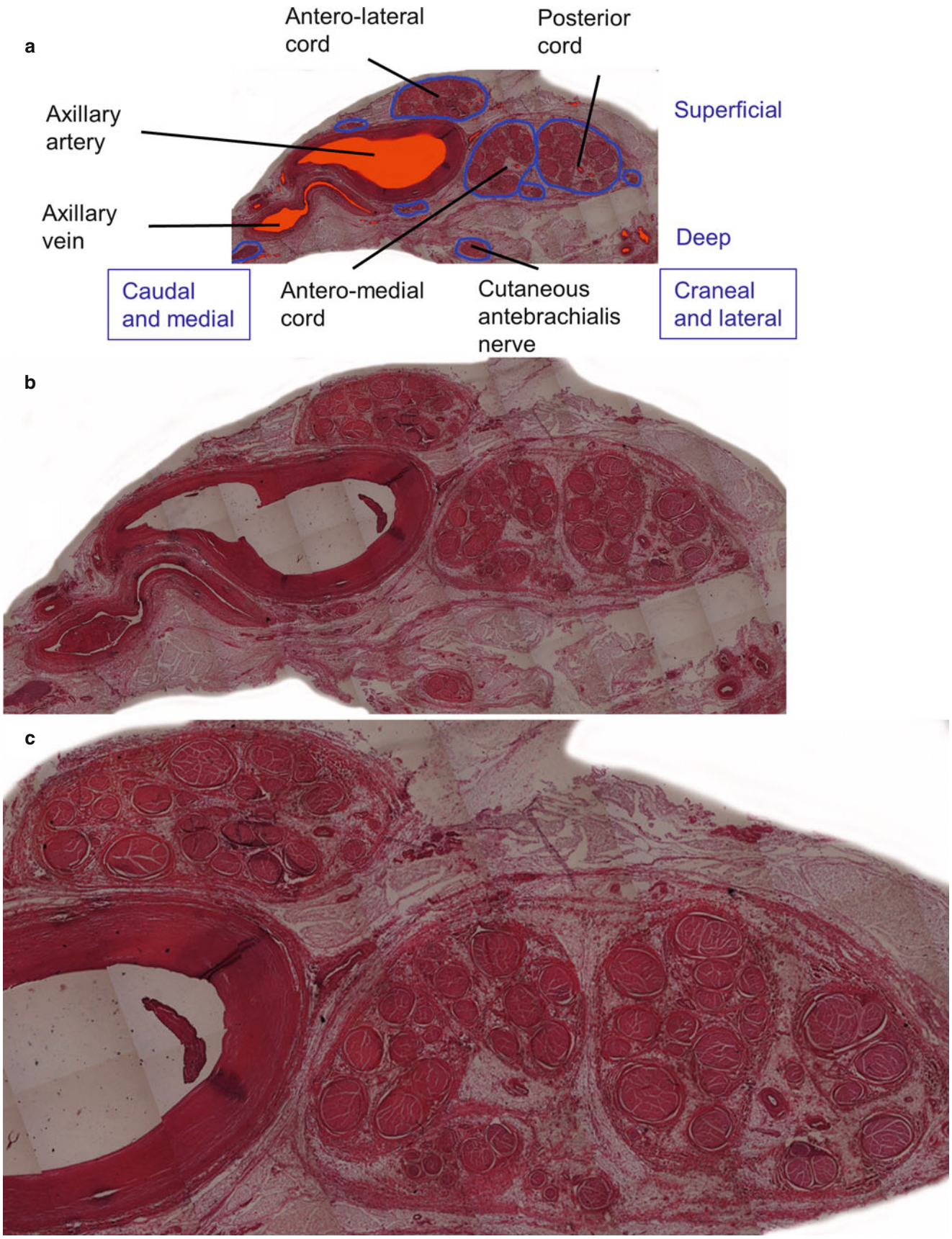

Fig. 8.14 (**a**) Brachial plexus, infraclavicular region at second part level (coracoid). (**b**): (**a**) at more magnification. (**c**) Detail of (**b**). Hematoxylin-eosin stained. Following section of a serially sectioned sample from Figs. 8.1 to 8.23

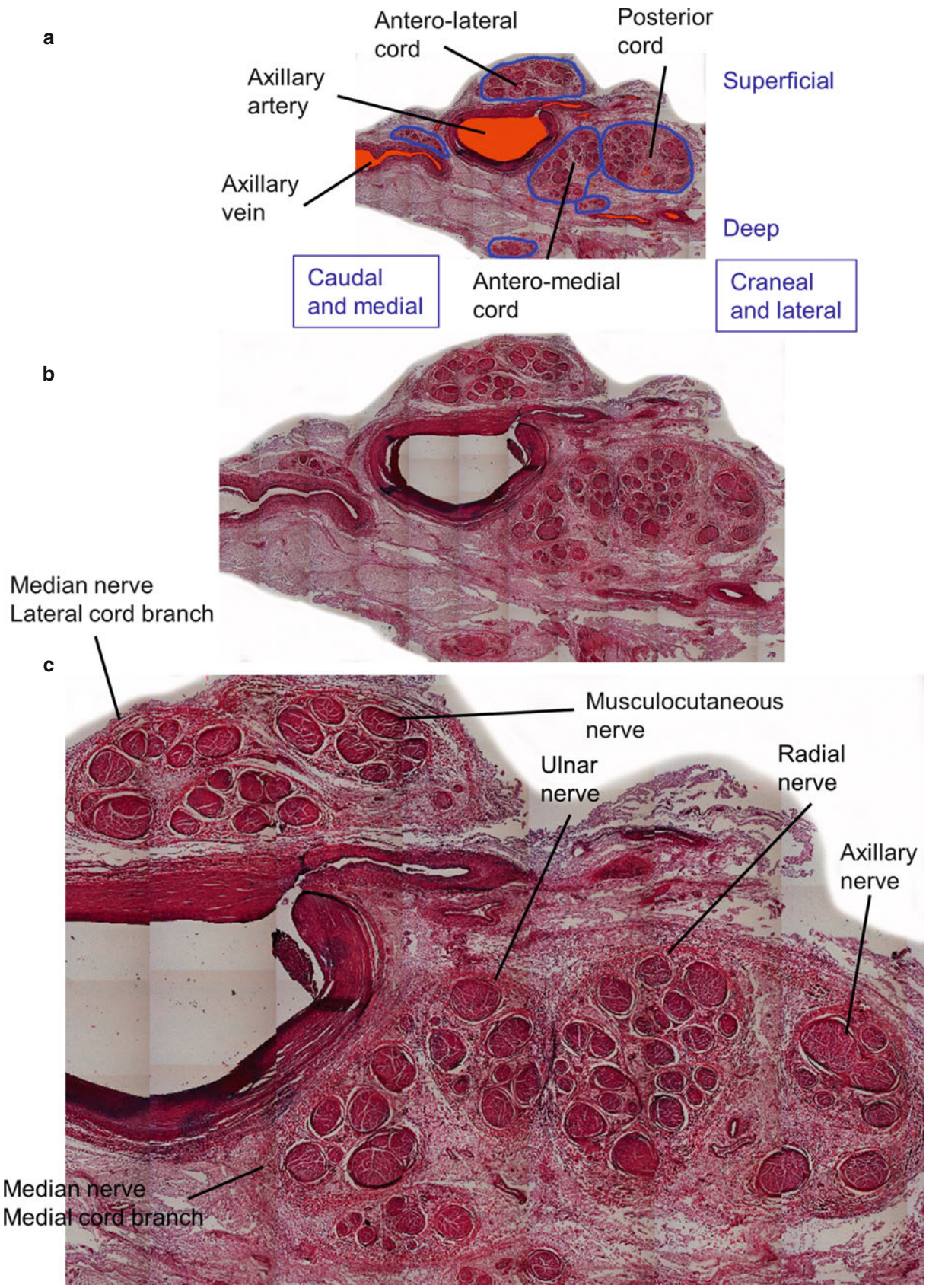

Fig. 8.15 (**a**) Brachial plexus, infraclavicular region at second part level (coracoid). (**b**): (**a**) at more magnification. (**c**) Detail of (**b**). Hematoxylin-eosin stained. Following section of a serially sectioned sample from Figs. 8.1 to 8.23

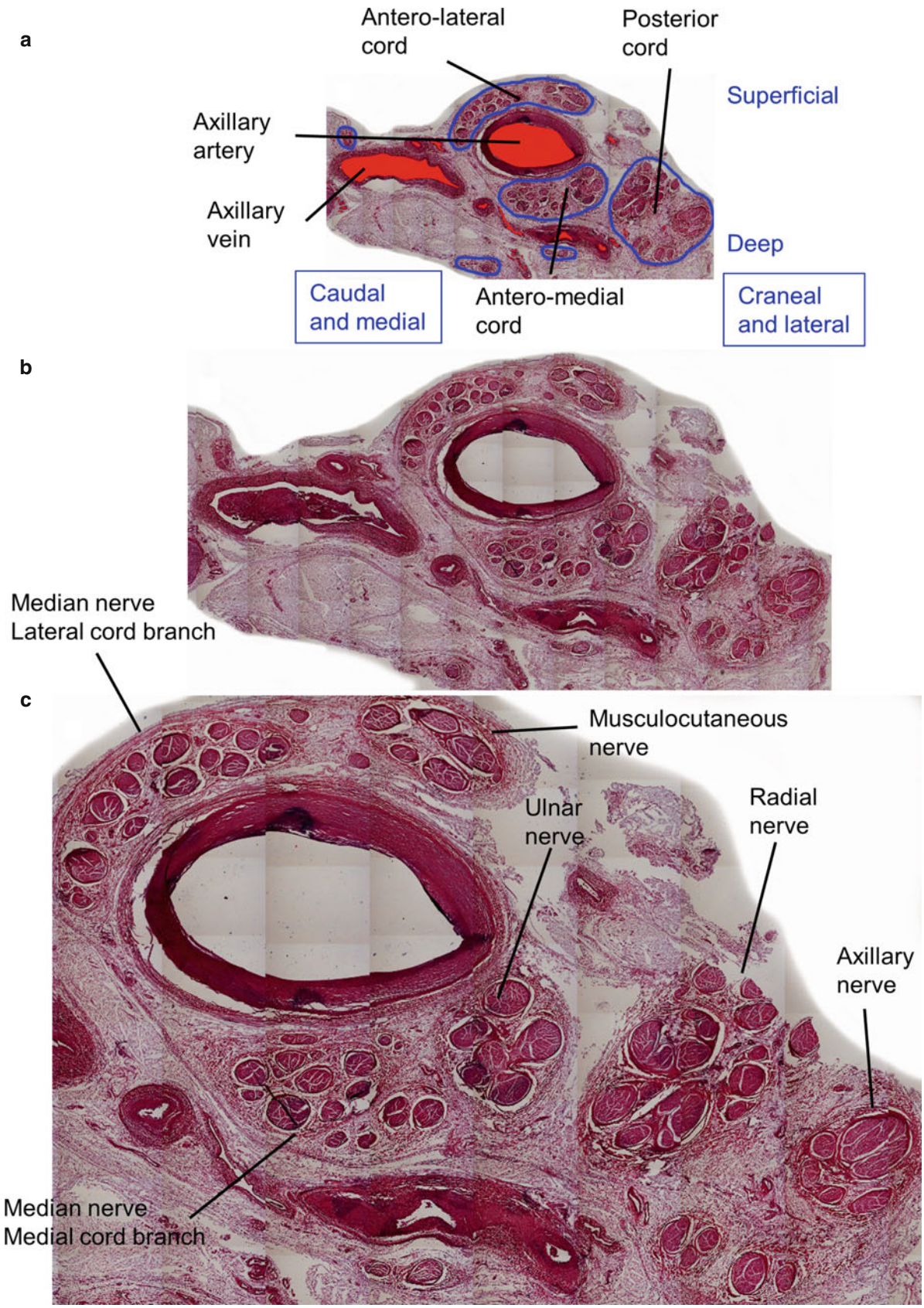

Fig. 8.16 (**a**) Brachial plexus, infraclavicular region at second part level (coracoid). (**b**): (a) at more magnification. (**c**) Detail of (**b**). Hematoxylin-eosin stained. Following section of a serially sectioned sample from Figs. 8.1 to 8.23

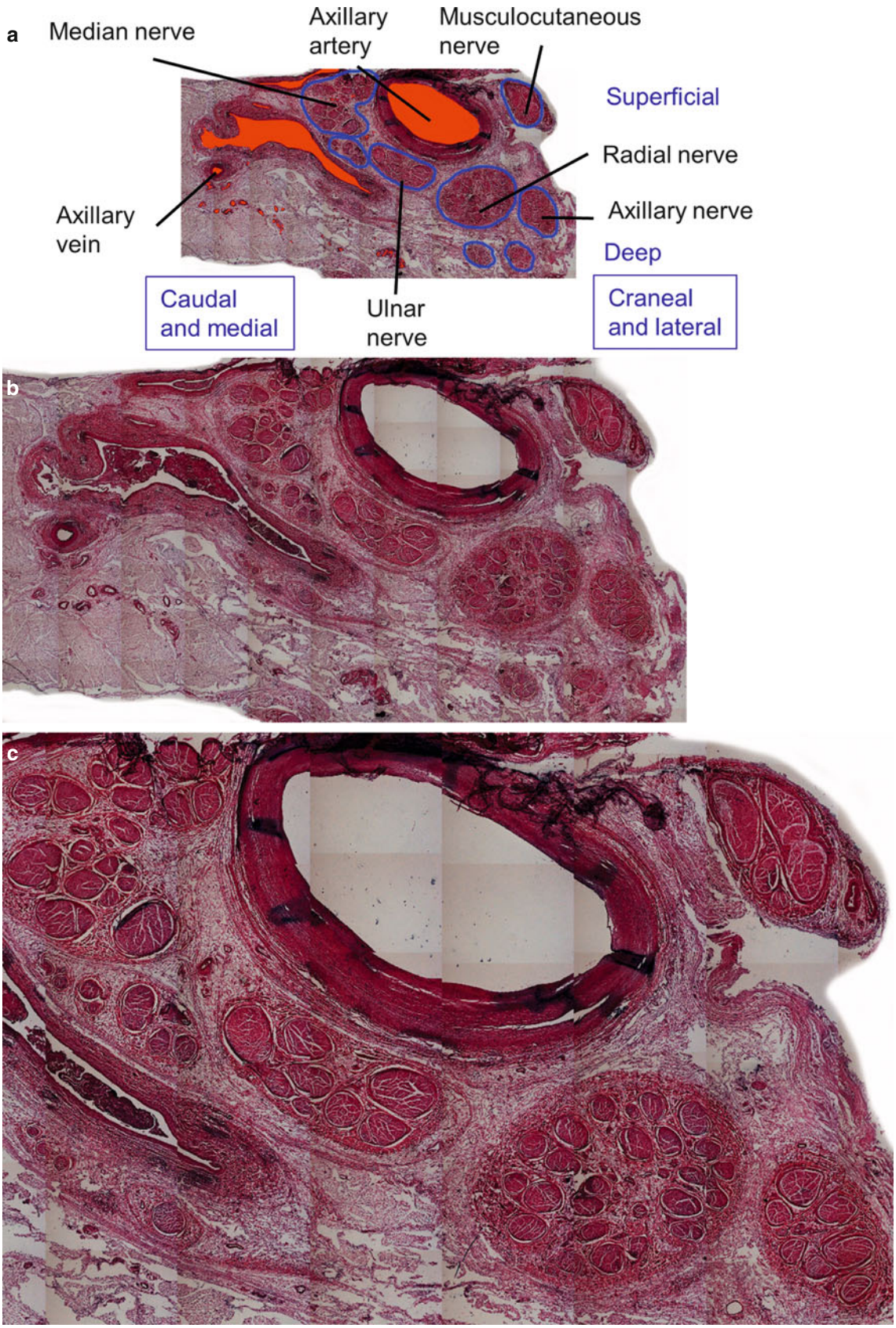

Fig. 8.17 (**a**) Brachial plexus, infraclavicular region at second part level (coracoid). (**b**): (**a**) at more magnification. (**c**) Detail of (**b**). Hematoxylin-eosin stained. Following section of a serially sectioned sample from Figs. 8.1 to 8.23

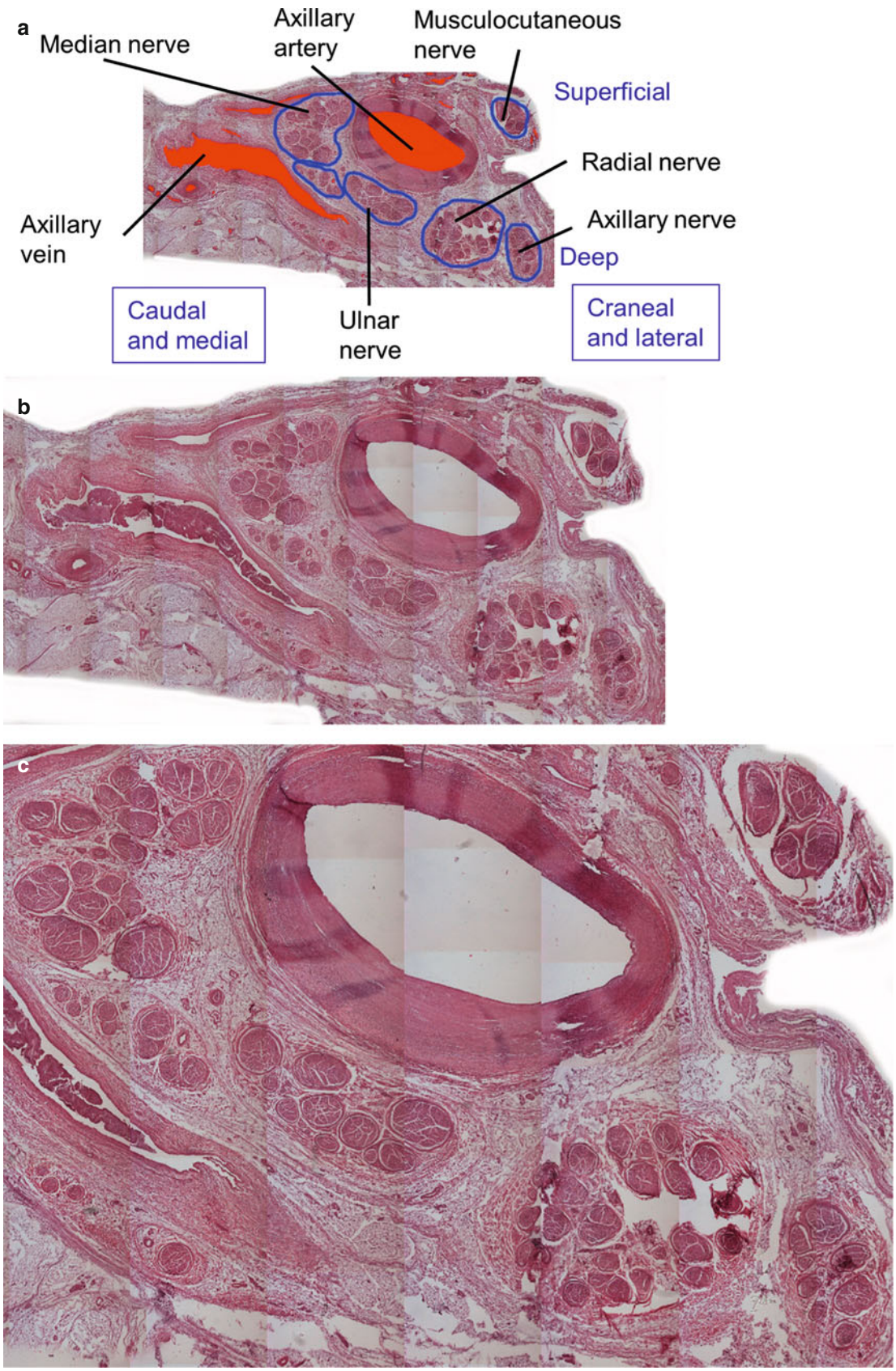

Fig. 8.18 (**a**) Brachial plexus, infraclavicular region at second part level (coracoid). (**b**): (**a**) at more magnification. (**c**) Detail of (**b**). Hematoxylin-eosin stained. Following section of a serially sectioned sample from Figs. 8.1 to 8.23

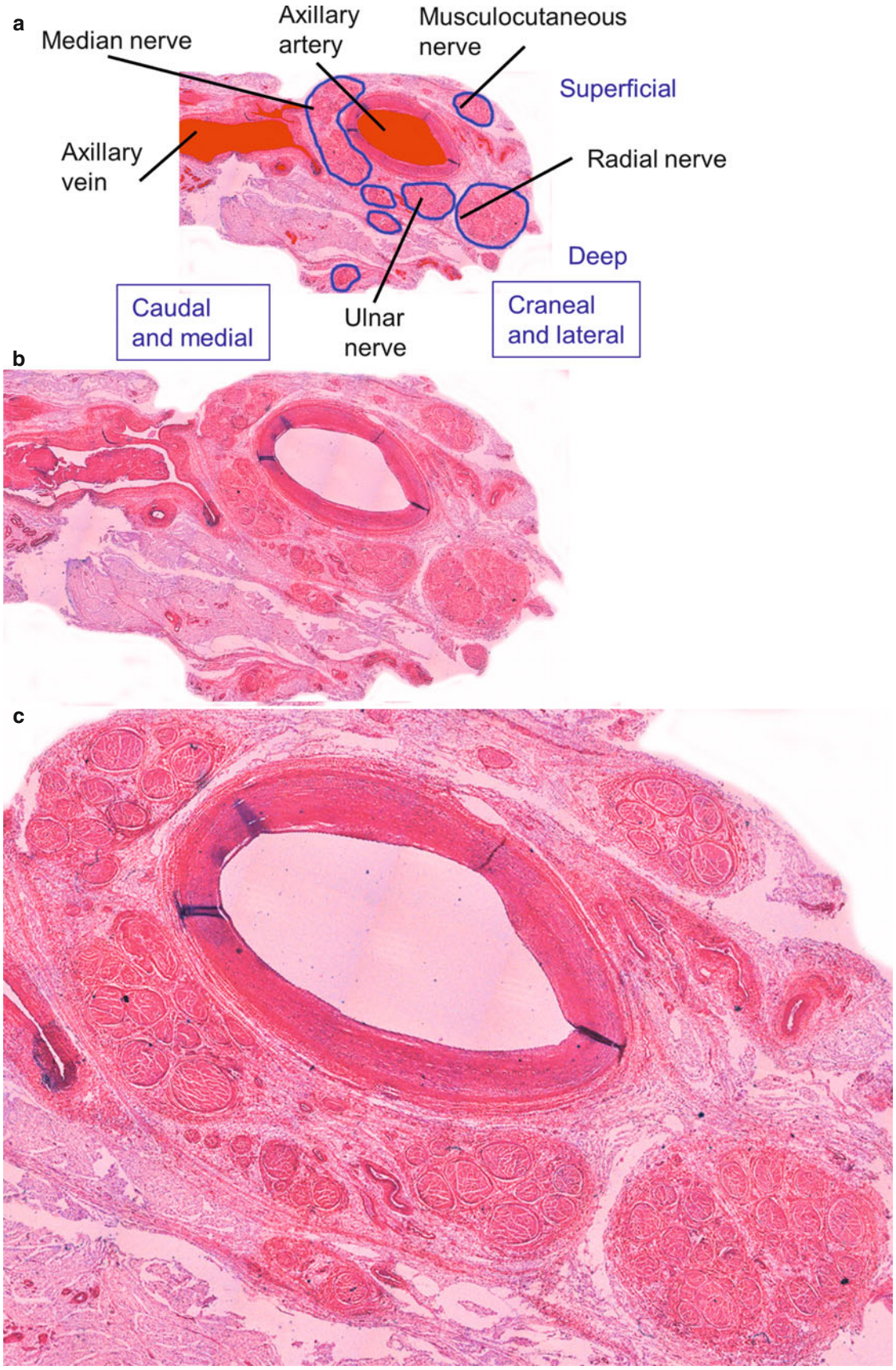

Fig. 8.19 (**a**) Brachial plexus, infraclavicular region at second part level (coracoid). (**b**): (**a**) at more magnification. (**c**) Detail of (**b**). Hematoxylin-eosin stained. Following section of a serially sectioned sample from Figs. 8.1 to 8.23

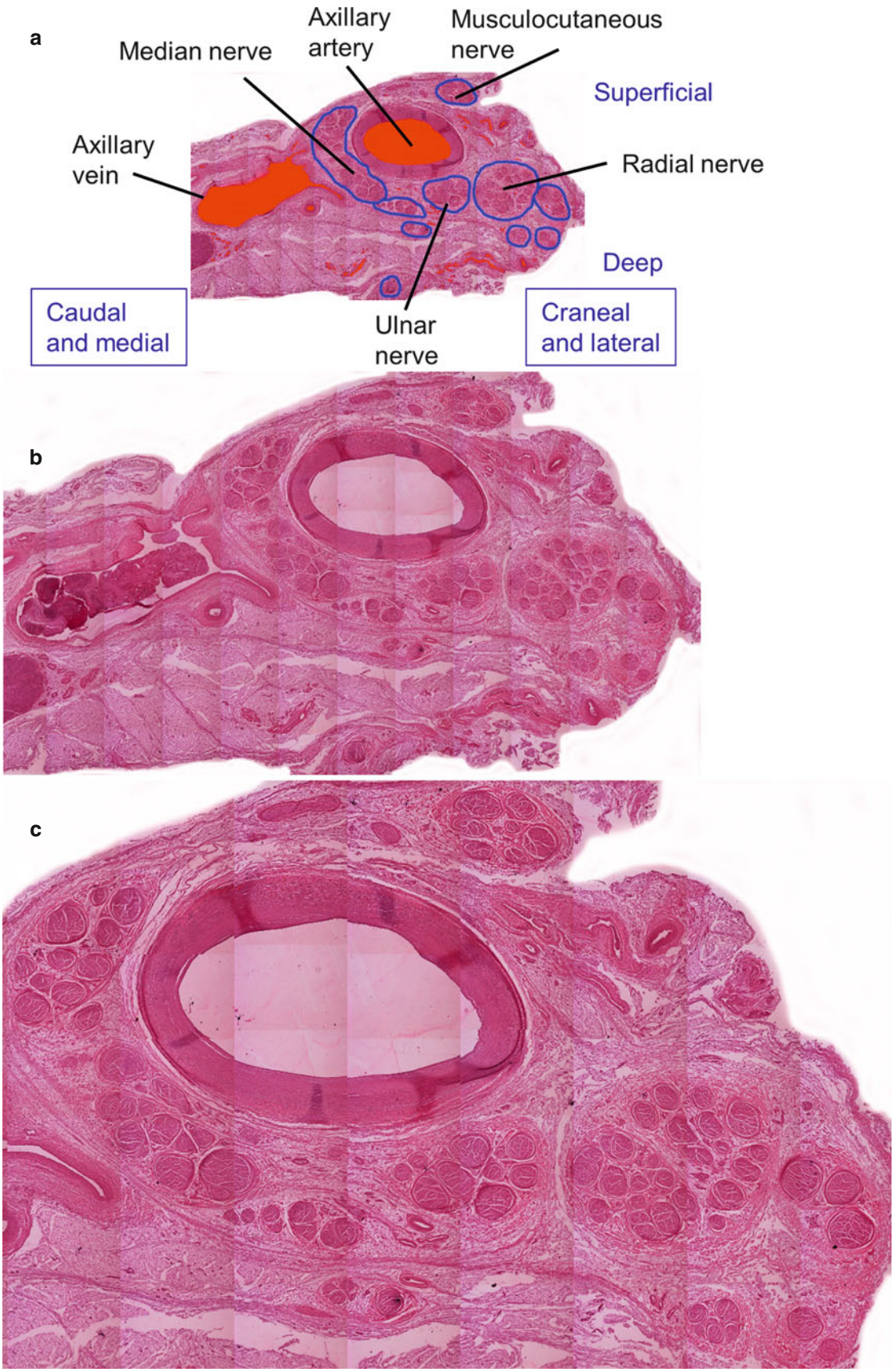

Fig. 8.20 (**a**) Brachial plexus, infraclavicular region at second part level (coracoid). (**b**): (**a**) at more magnification. (**c**) Detail of (**b**). Hematoxylin-eosin stained. Following section of a serially sectioned sample from Figs. 8.1 to 8.23

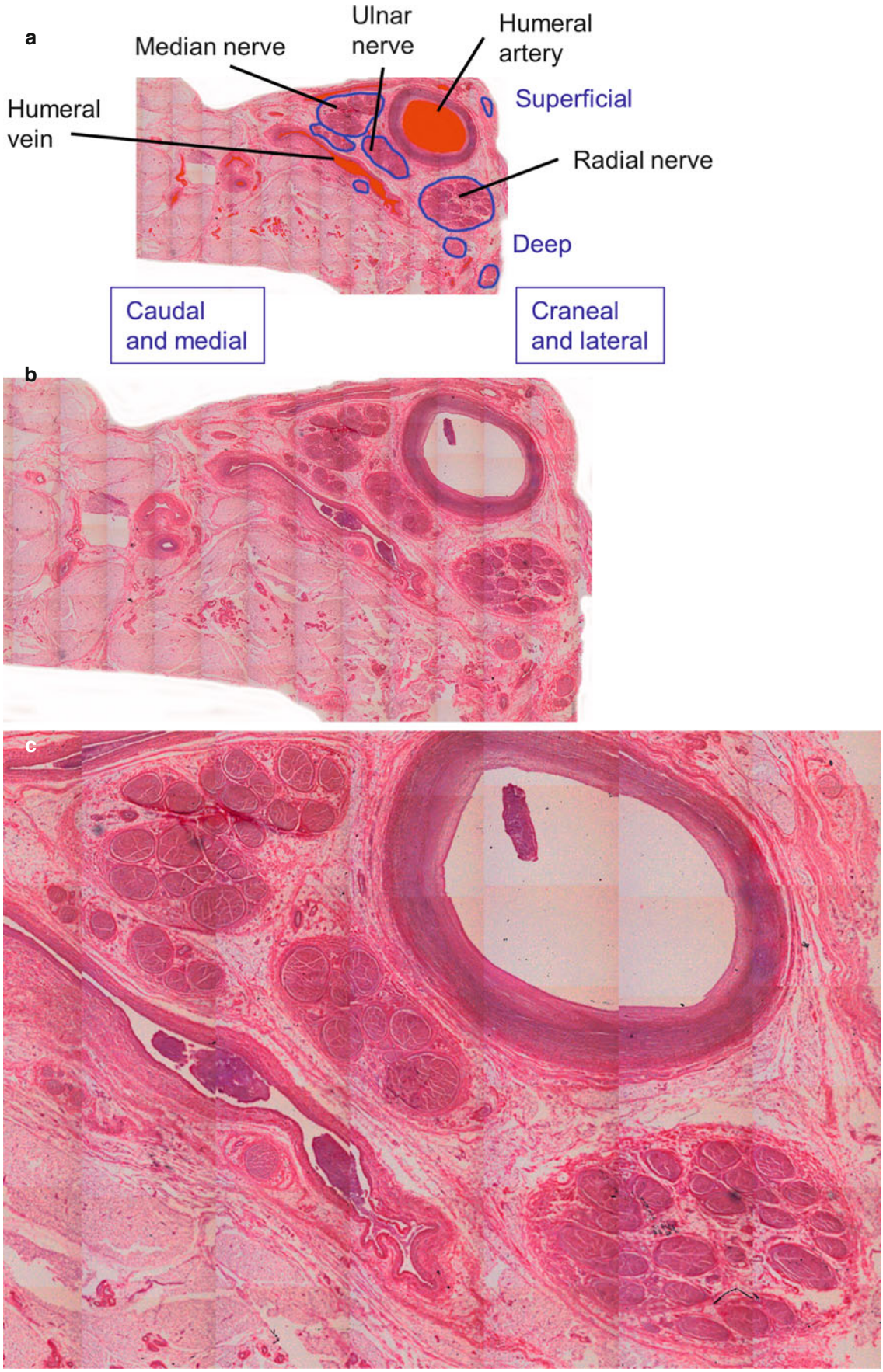

Fig. 8.21 (**a**) Brachial plexus, axillary region. (**b**): (**a**) at more magnification. (**c**) Detail of (**b**). Hematoxylin-eosin stained. Following section of a serially sectioned sample from Figs. 8.1 to 8.23

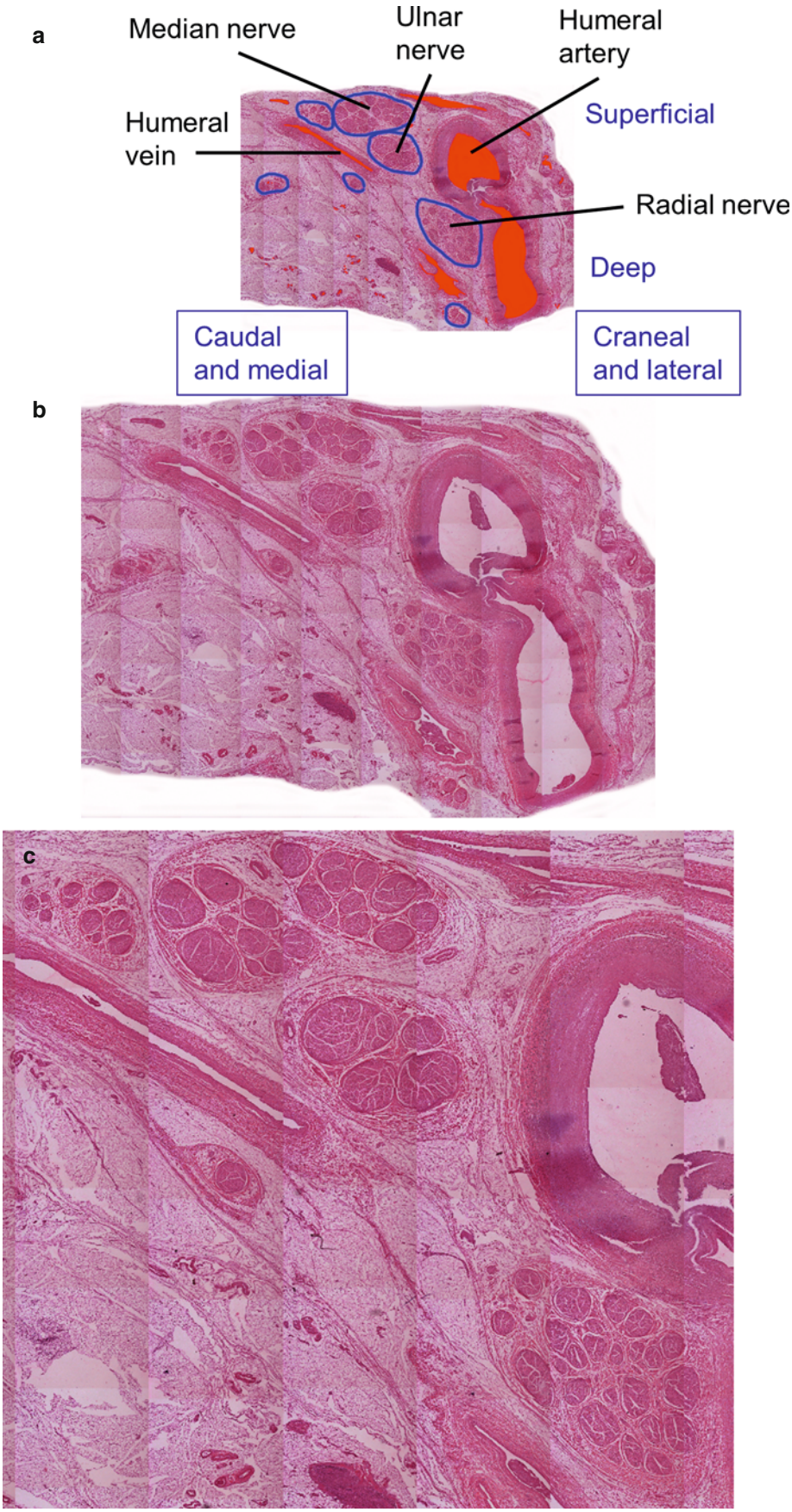

Fig. 8.22 (**a**) Brachial plexus, axillary region. (**b**): (**a**) at more magnification. (**c**) Detail of (**b**). Hematoxylin-eosin stained. Following section of a serially sectioned sample from Figs. 8.1 to 8.23

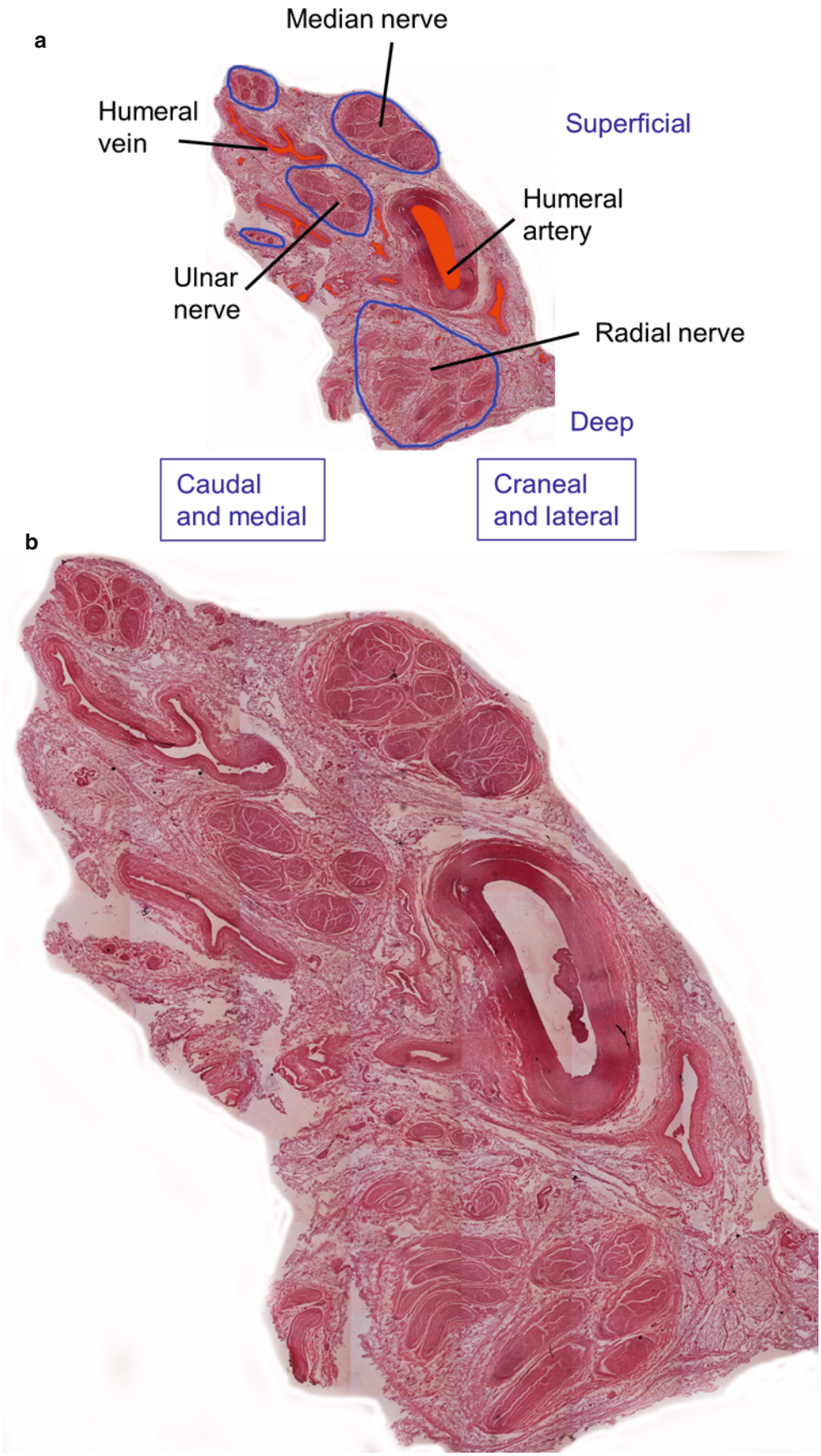

Fig. 8.23 (**a**) Brachial plexus, axillary region. (**b**): (**a**) at more magnification. (**c**) Detail of (**b**). Hematoxylin-eosin stained. Last section of a serially sectioned sample from Figs. 8.1 to 8.23

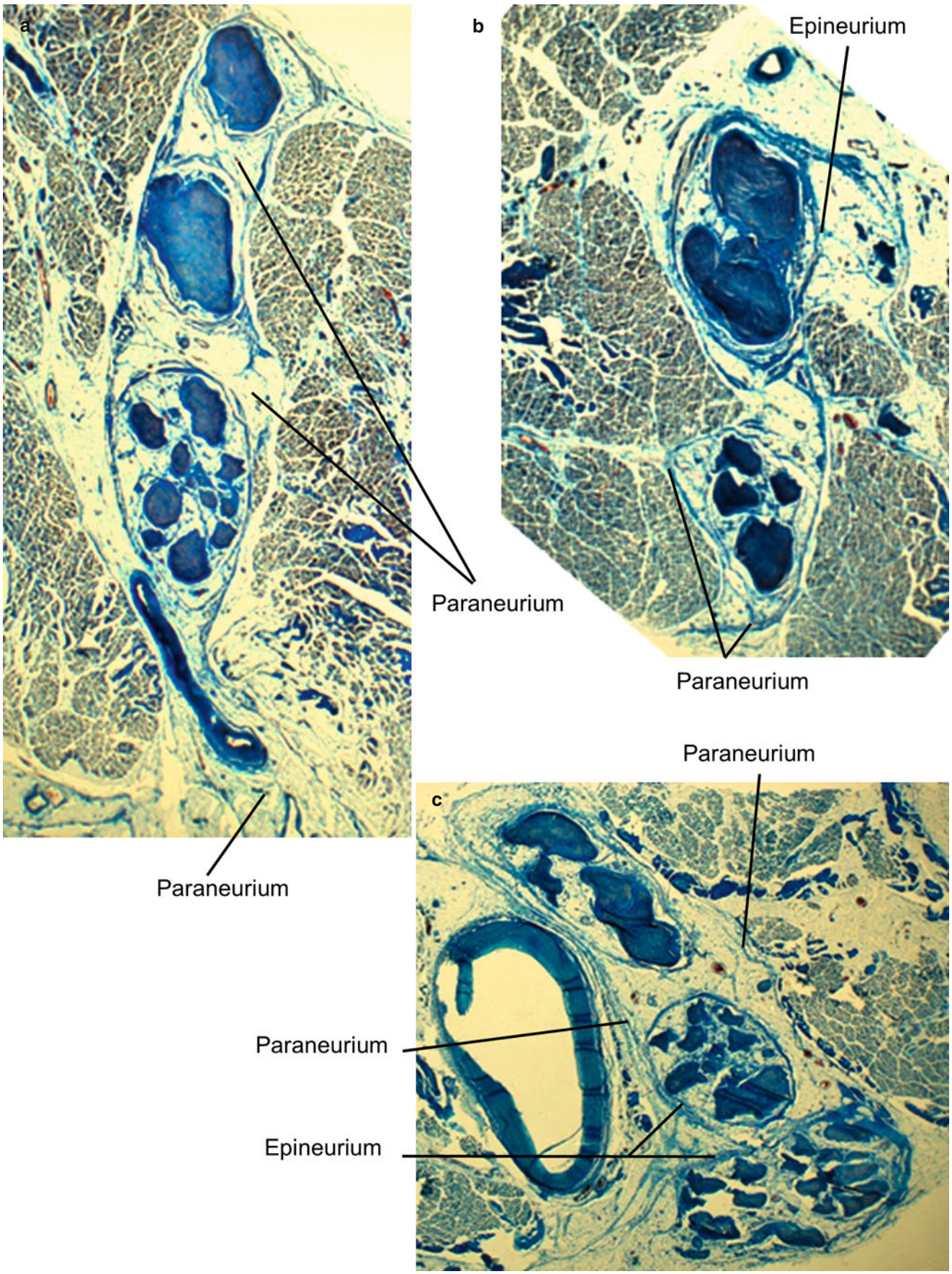

Fig. 8.24 Details of internal structure of nerve root in interscalenic region. (**a**) Detail obtained from Fig. 8.1, (**b**) Detail obtained from Fig. 8.2a, (**c**) Detail obtained from Fig. 8.2b. Masson's trichrome stained

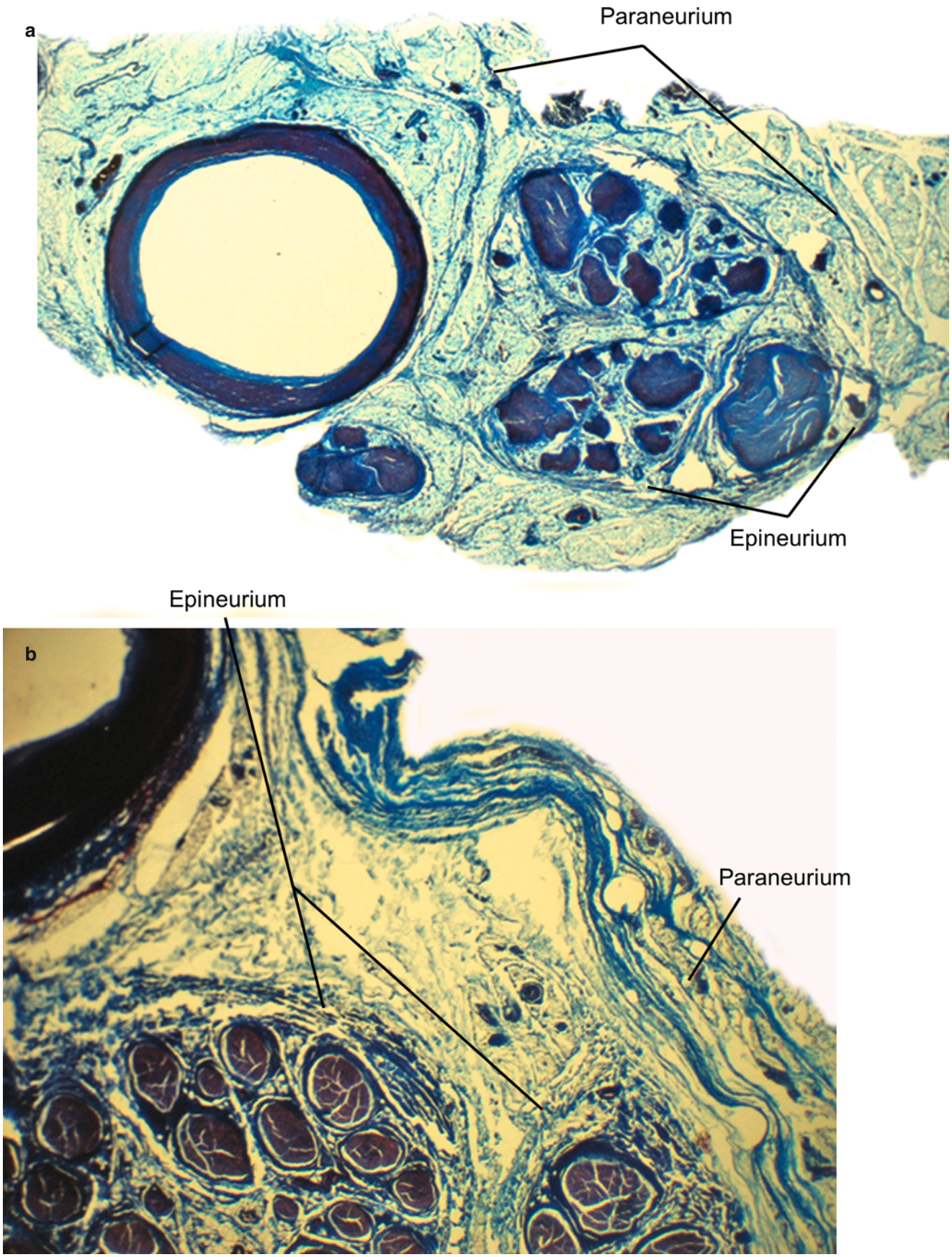

Fig. 8.25 (**a**, **b**) Details of internal structure of nerve trunks in supraclavicular region obtained from different samples. Masson's trichrome stained

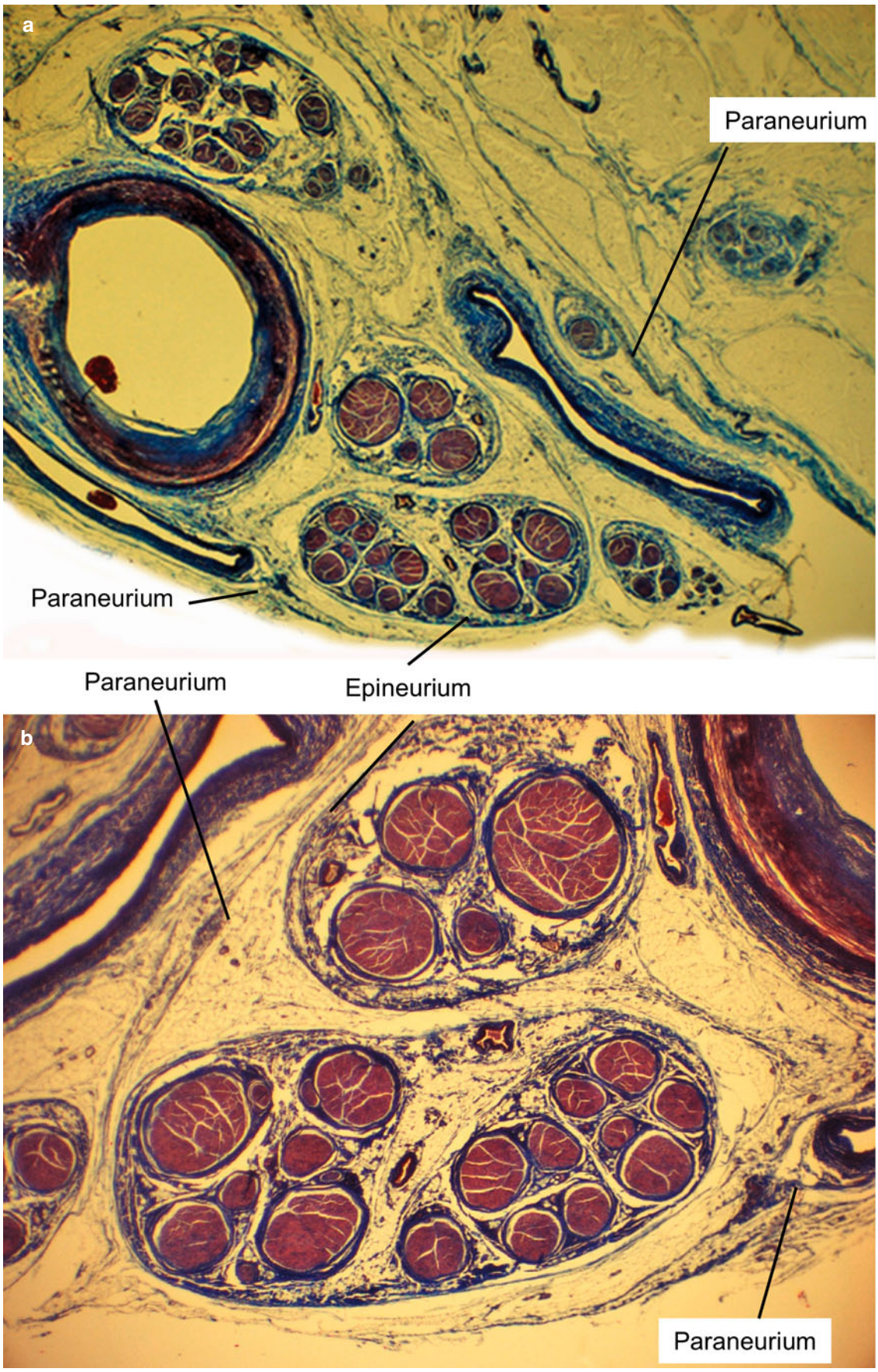

Fig. 8.26 (**a**, **b**) Details of internal structure of nerves in infraclavicular region. (**b**) Detail at more magnification from (**a**). Masson's trichrome stained

References

1. Reina MA, De Andrés JA, Hernández JM, Arriazu Navarro R, Durán Mateos EM, Prats-Galino A. Successive changes in extraneural structures from the subarachnoid nerve roots to the peripheral nerve, influencing anesthetic block, and treatment of acute postoperative pain. Eur J Pain Suppl. 2011;5:377–85.
2. Reina MA, Arriazu R, Collier CB, Sala-Blanch X, Izquierdo L, de Andrés J. Electron microscopy of human peripheral nerves of clinical relevance to the practice of nerve blocks. A structural and ultrastructural review based on original experimental and laboratory data. Rev Esp Anestesiol Reanim. 2013;60:552–62.
3. Yokoyama I. Study on the intraneural topography of the brachial plexus [in Japanese]. Nihon Seikeigeka Gakkai Zasshi. 1989;63:1085–102.
4. Yokoyama I, Matsuda H, Hashimoto T, Kureya S, Shimazu A. Intraneural topography of the brachial plexus. Microscopic dissection in human cadavers. J Jpn Soc Surg Hand. 1986;3:138–45.
5. Sunderland S, Marshall RD, Swaney WE. The intraneural topography of the circumflex musculocutaneous and obturator nerves. Brain. 1959;82:116–29.
6. Sunderland S. The intraneural topography of the radial, median and ulnar nerves. Brain. 1945;68:243–55.